University of Bath

A study of L-band scintillations and total electron content at an equatorial station, Lagos, Nigeria

A. O. Adewale,[1] E. O. Oyeyemi,[1] A. B. Adeloye,[1] C. N. Mitchell,[2] J. A. R. Rose,[2] and P. J. Cilliers[3]

[1] In this paper we present the first results from measurements of scintillation and total electron content (TEC) from an equatorial station, Lagos (Latitude 6.5°N, Longitude 3.4°E, magnetic latitude 3.03°S), Nigeria, using a Novatel GSV4004B GPS ionospheric scintillation and TEC monitor. Details are presented for data collected between February 2010 and August 2010. The results show that the presence of some large scale depletions of TEC or plasma bubbles may be noted during the evening hours and that TEC depletions correspond to increased rate of change of TEC (ROT). This confirms that plasma bubbles are associated with large scale irregularities. It is also established that enhanced amplitude scintillation (S_4) corresponds quite well with TEC depletions and increases in ROT. The diurnal and seasonal percentage occurrence for different levels of scintillation activity has peaks in the equinox months (March and April) at 23:00 LT.

Citation: Adewale, A. O., E. O. Oyeyemi, A. B. Adeloye, C. N. Mitchell, J. A. R. Rose, and P. J. Cilliers (2012), A study of L-band scintillations and total electron content at an equatorial station, Lagos, Nigeria, *Radio Sci.*, *47*, RS2011, doi:10.1029/2011RS004846.

1. Introduction

[2] In recent years, a major concern of the equatorial ionospheric communication scientists has been the understanding of the structure and formation of small-scale ionospheric irregularities that cause degradation of radio signals on transionospheric links. These irregularities are formed at the bottom of F region during post-sunset period due to the Rayleigh-Taylor gravitational instability mechanism. During post-sunset, the lower regions of the F-layer recombine more rapidly than the upper regions, leading to an unstable situation similar to a heavy fluid being supported on a lighter fluid. This situation eventually leads to the formation of plasma depleted flux tubes (plasma bubbles) which are forced upwards through the denser upper regions marking the development of post-sunset equatorial spread F [*Abdu et al.*, 2009]. As the bubbles grow, steep density gradients on the walls cause smaller irregularities to form. These smaller irregularities are responsible for scintillations. According to *Basu et al.* [1999], amplitude scintillations on GPS L1 signals are caused by irregularities of about 400 m. Ionospheric researchers and communication engineers [*Wanninger*, 1993; *Doherty et al.*, 1994; *Aarons et al.*, 1996; *Mitchell et al.*, 1997; *Groves et al.*, 1997; *Basu et al.*, 1999; *Andreeva et al.*, 2000; *Wernik et al.*, 2003; *Dabas and Kersley*, 2003] have focused attention on the effects of ionospheric scintillation on radio signals propagating through the ionosphere from the satellites of the Global Navigation Satellite System (GNSS).

[3] The Global Positioning System (GPS), the U.S. component of the GNSS, is a satellite-based navigation system consisting of a network of 24 satellites in 6 orbital planes with 4 satellites in each plane. The GPS satellites orbit at an altitude of about 20,200 km with an orbital plane inclination of 55 degrees to the Earth's equator. Each satellite transmits signals at two frequencies, 1575.42 MHz (L1) and 1227.60 MHz (L2).

[4] GPS signals are delayed relative to the speed of light in vacuum as they propagate through the ionized region of the ionosphere due to the presence of free electrons. The total electron content (TEC) is the integral of electron density along the raypath between the ground stations and satellites. Observations from a dual frequency GPS receiver show a slow variation in TEC for several minutes or hours during undisturbed ionospheric conditions. During scintillations satellite communication systems produce error messages and the accuracy of GPS navigation decreases. As a result, an understanding of the effect of the ionospheric irregularities on GPS signals is required for correct interpretation of GPS-derived TEC thereby providing ionospheric information, and also, providing a better understanding of the temporal and spatial variation of the ionosphere as it affects GPS navigation systems, satellite communications and radio wave communications.

[1]Department of Physics, University of Lagos, Lagos, Nigeria.
[2]Invert Centre for Imaging Science, Department of Electronic and Electrical Engineering, University of Bath, UK.
[3]South African National Space Agency Space Science, Hermanus, South Africa.
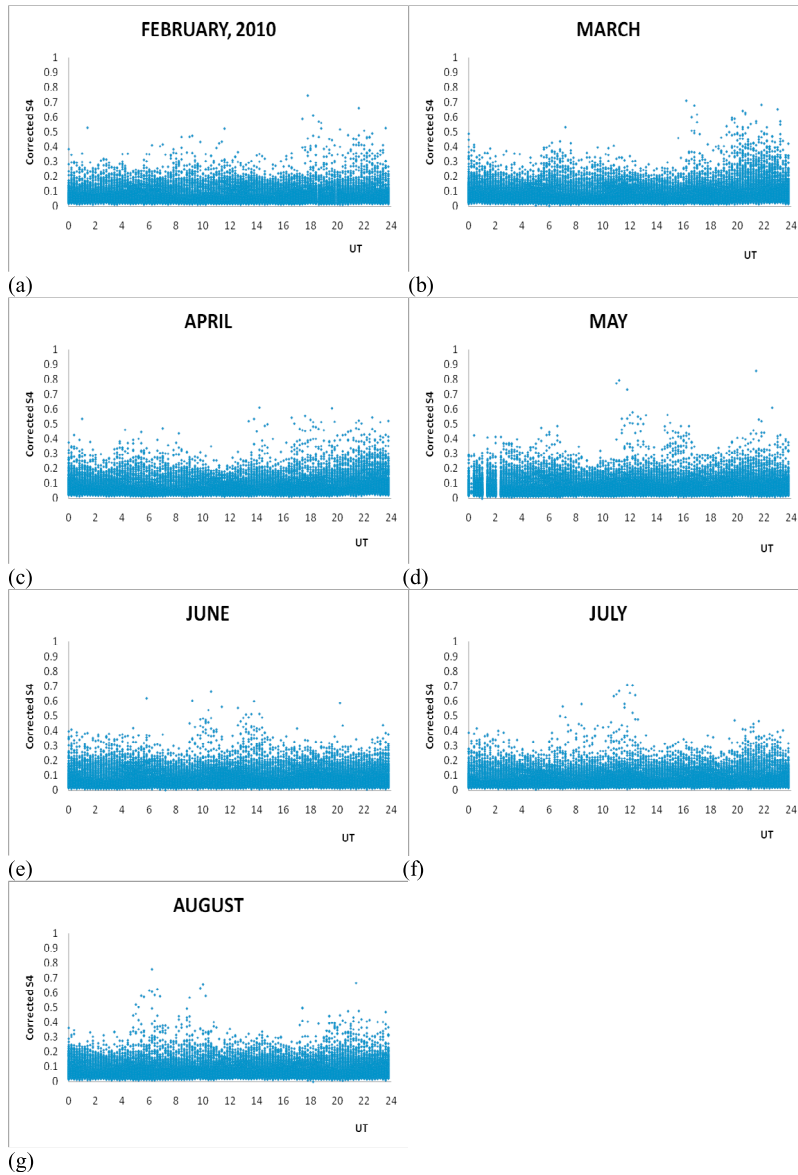
Figure 1. Month-to-month variations of corrected amplitude scintillation occurrence observed at Lagos from February to August 2010 (LT = UT + 1 h).
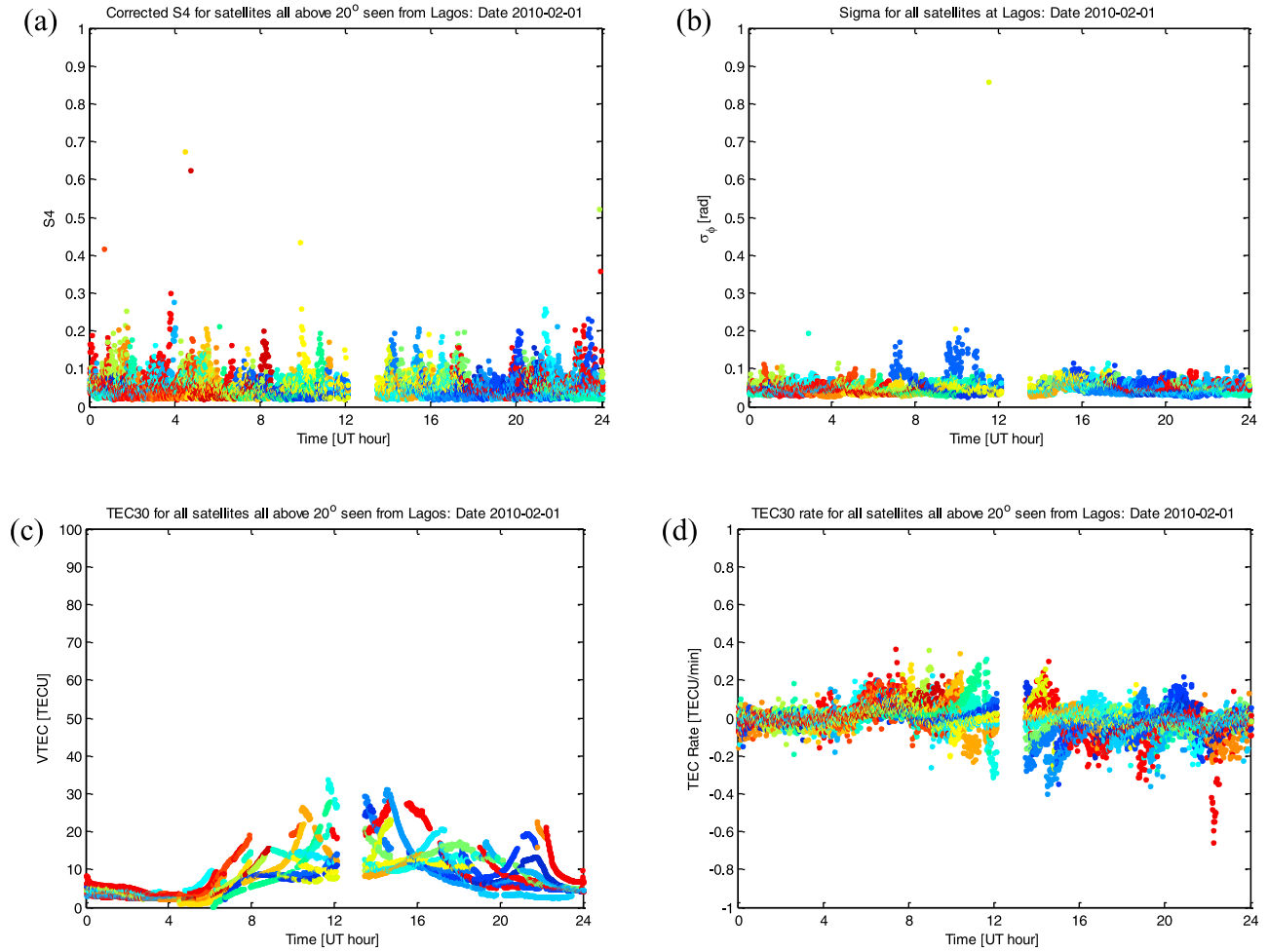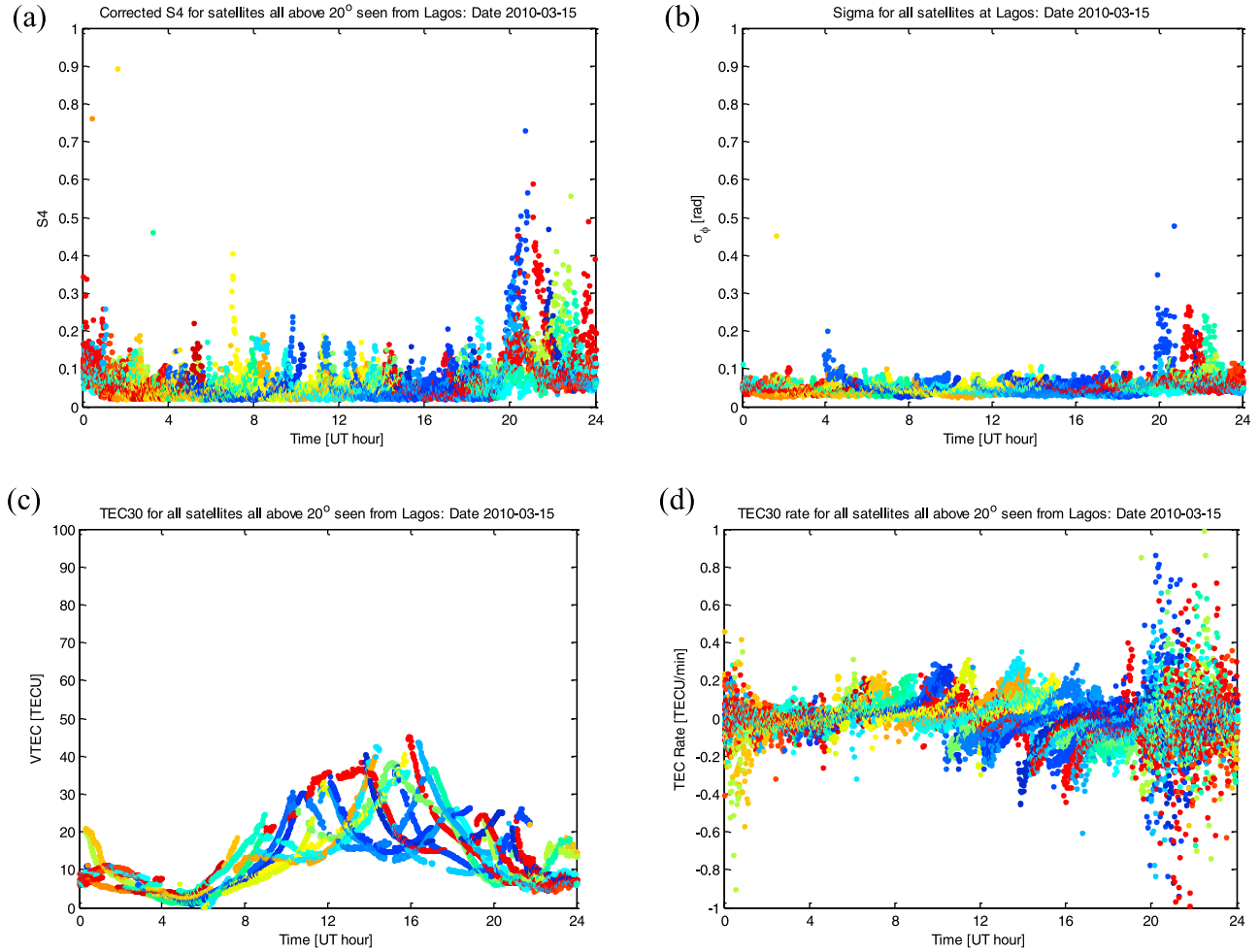
Figure 2. Plots of (a) S$_4$, (b) sigma, (c) VTEC, and (d) TEC rate for 1 February 2010 (non-scintillation day) (LT = UT + 1 h). (Note that the gap around 12:00 UT is due to a power cut.)

[5] When a radio wave propagates through a medium containing plasma instability, the signal suffers amplitude and phase distortions. Ionospheric scintillations are rapid variations in the amplitude and phase of radio signals due to electron density irregularities in the ionosphere. The amplitude scintillation index (S$_4$) is computed over 1 min as the standard deviation of the detrended signal intensity (I) normalized by its mean value and is defined as the total S$_4$:

$$S_{4T} = \sqrt{\frac{\langle I^2 \rangle - \langle I \rangle^2}{\langle I \rangle^2}}. \tag{1}$$

[6] The phase scintillation index (σ_φ) is defined as the standard deviation of the detrended carrier phase from received GPS signals, averaged over 1 min. If the intensity of the irregularity is low, only the phase and angle of arrival of the signals are changed. If the irregularity intensity is strong, the amplitude of the signal also varies. Basically, both amplitude and phase scintillation occurred when the ionospheric disturbance is strong.

[7] Several studies have shown that ionospheric scintillations show strong diurnal, seasonal, geographic and solar cycle variations [*Basu and Basu*, 1985; *Groves et al.*, 1997; *Andreeva et al.*, 2000]. It is most severe during the evening hours at equatorial latitudes (moderate at high latitudes and generally absent at midlatitudes) and during years of high solar activity. Scintillation affects the accuracy of the GPS receiver pseudorange and carrier phase measurements. It can also result in complete loss of phase lock on a GPS satellite which could result in degradation of position estimate. Studies from various groups [*Basu and Basu*, 1985; *Groves et al.*, 1997; *Andreeva et al.*, 2000; *Huang et al.*, 2001; *Dandekar and Groves*, 2004] have shown that scintillations predominantly occur in a band approximately ±20° of the magnetic equator and in the polar and auroral regions. Results from these studies have also shown that equatorial scintillations are produced by irregularities created by bubbles of low density plasma that form at the bottom of the F region ionization layer and penetrate upwards through the denser topside ionosphere, just after sunset. These low density bubbles, which eventually form into plumes at the magnetic equator (about ±20° latitudes) become unstable and develop into small-scale irregular density structures, and

Figure 3. Plots of (a) S$_4$, (b) sigma, (c) VTEC, and (d) TEC rate for 15 March 2010 (LT = UT + 1 h).

degrade communications and navigation in the equatorial region.

[8] Despite present studies on scintillations and ionospheric tomography elsewhere, significant work has not been carried out in the equatorial region of the African continent due to paucity of GPS scintillation data. Because results have shown that scintillations predominantly occur at the equatorial region, there have been several efforts, in recent times, to install GPS receivers in the equatorial regions of Africa, by several organizations and institutions. Such efforts include the installation of two GPS receivers in the Department of Physics, University of Lagos, Nigeria by Invert Centre, University of Bath, and Boston College, United State of America. Also, the Scintillation Network Decision Aid (SCINDA) installed GPS scintillation receivers in a number of countries (including Nigeria) along the equatorial region of Africa.

[9] The aim of this present work is to document a study, *albeit*, a preliminary one, of the TEC and S$_4$ parameters over Lagos, Nigeria.

2. Data and Methodology

[10] The GPS observation data used for this work was obtained from the GSV4004B GPS Ionospheric Scintillation

and TEC Monitor (GISTM) installed at the Department of Physics, University of Lagos (6.5°N, 3.4°E; magnetic latitude 3.03°S), Nigeria. The GPS receiver can track up to 11 GPS satellites at the L1 and L2 frequency simultaneously and measures both phase and amplitude at a 50-Hz rate for each satellite tracked on L1 and calculates the amplitude and phase scintillation index in real time from the receiver-detrended scintillation data. The raw amplitude measurements are detrended (by normalization), with a 6th-order Butterworth low-pass filter output. The data analyzed was collected over the period February 2010 to August 2010. The software supplied with the GSV4004B monitor computes the S$_{4T}$ and the ambient noise correction as follows:

$$S_{4No} = \sqrt{\frac{100}{S/N_o}\left[1 + \frac{500}{19S/N_o}\right]} \tag{2}$$

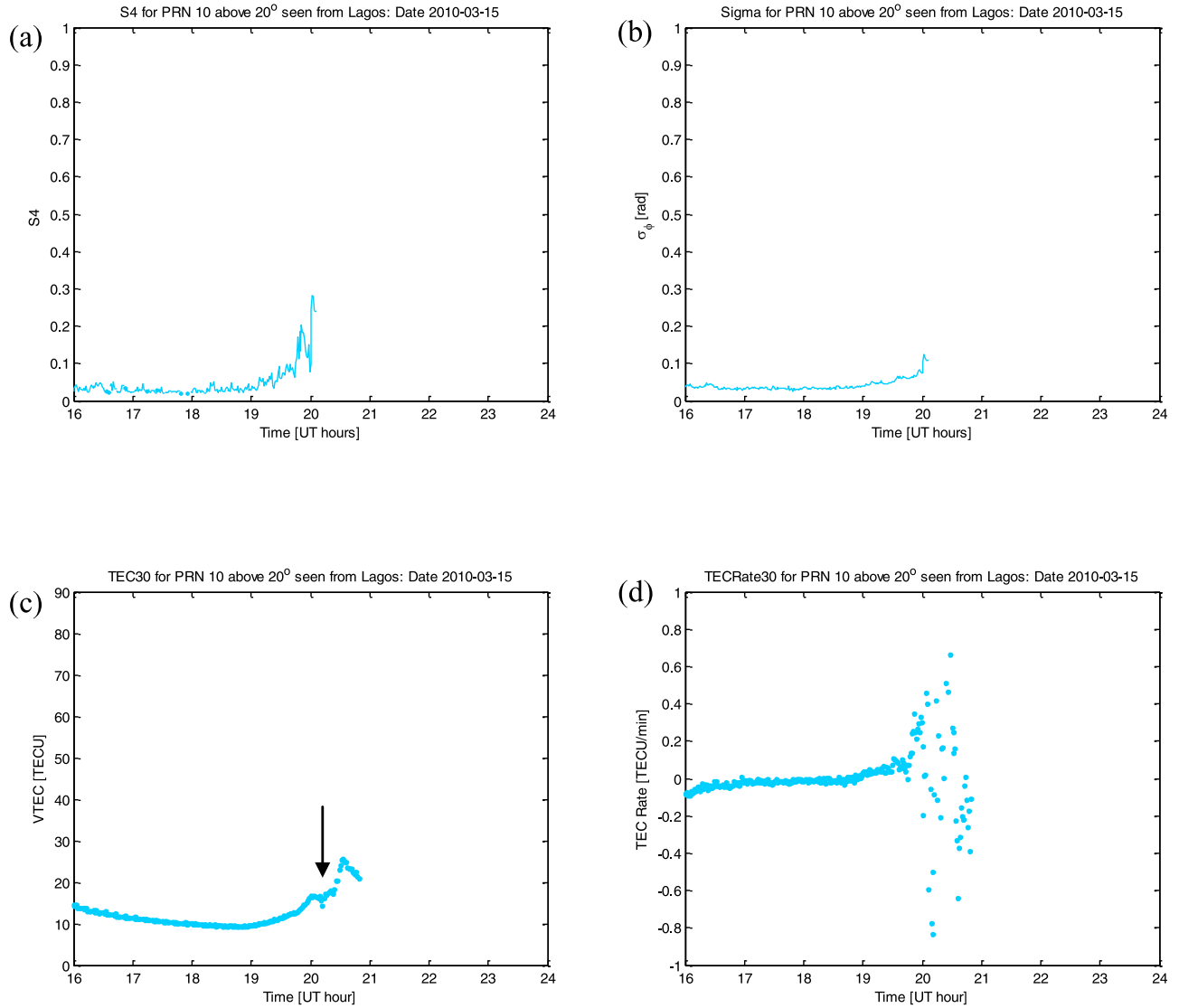where S/N_o is the signal-to-noise ratio averaged over a 60-s interval.

[11] According to *Dubey et al.* [2006], the corrected S$_4$ with the effects of ambient noise removed is computed as follows:

$$S_4 = \sqrt{S_{4T}^2 - S_{4No}^2}. \tag{3}$$
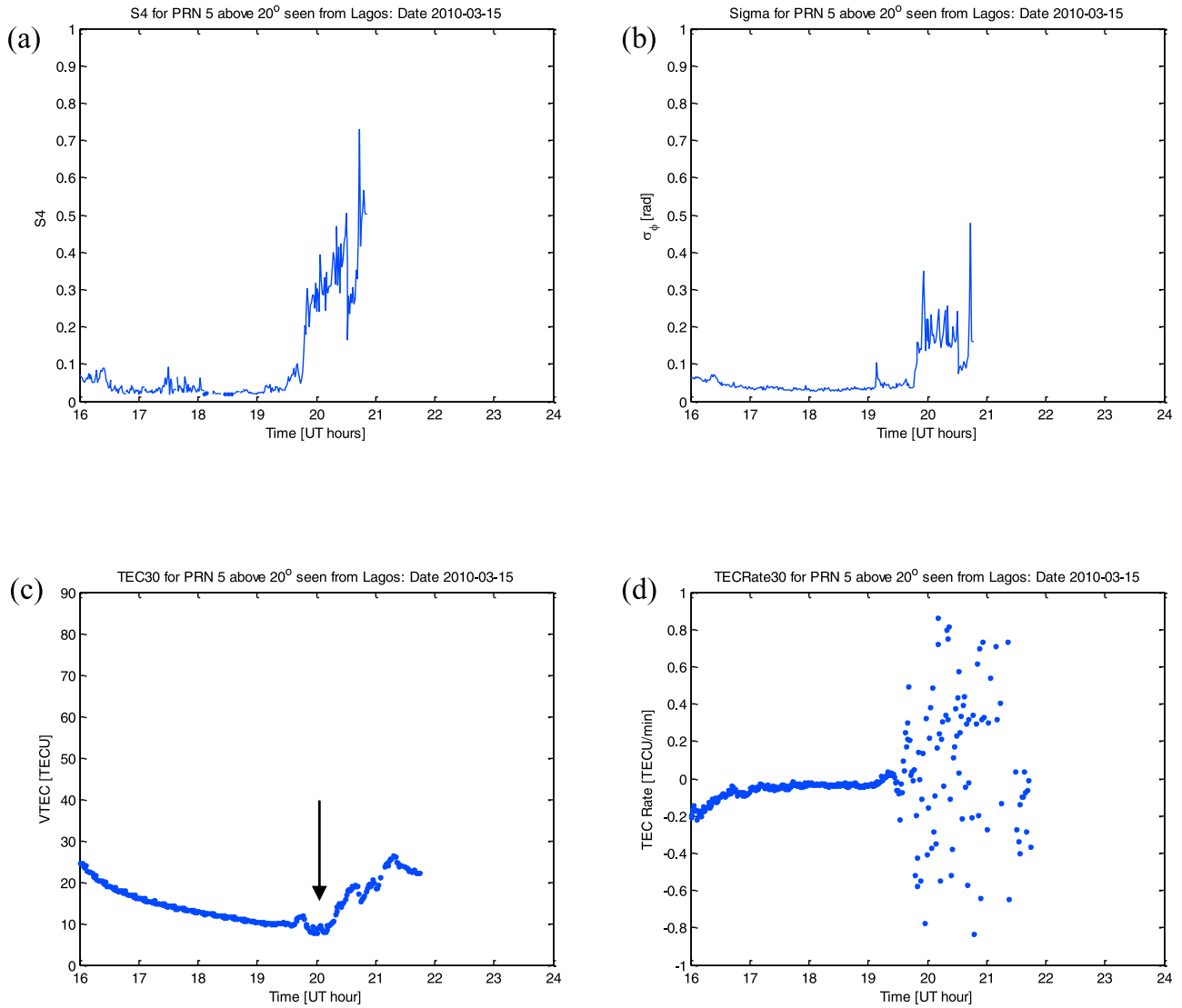
Figure 4. Plots of (a) S$_4$, (b) sigma, (c) VTEC, and (d) TEC rate for PRN 5 (LT = UT + 1 h). (The arrow indicates the presence of plasma bubble.)

(a)

S4 for PRN 10 above 20° seen from Lagos: Date 2010-03-15

(b)

Sigma for PRN 10 above 20° seen from Lagos: Date 2010-03-15

(c)

TEC30 for PRN 10 above 20° seen from Lagos: Date 2010-03-15

(d)

TECRate30 for PRN 10 above 20° seen from Lagos: Date 2010-03-15

Figure 5. Plots of (a) S_4, (b) sigma, (c) VTEC, and (d) TEC rate for PRN 10 (LT = UT + 1 h). (The arrow indicates the presence of plasma bubble.)

[12] The software computes five values of σ_φ for every 60-s, respectively over 1, 3, 10, 30 and 60-s intervals. The 60-s σ_φ values are used in our analysis.

[13] We used the parsing program, (Parseismr.exe) to convert binary format data records to a comma-delimited format. The phase scintillation data collected before the phase detrending filter converged were eliminated by deleting data with Lock Times less than 240 s and data with $\sigma_\varphi > 2$. This will eliminate confusion with legitimate scintillation events.

[14] We converted the slant TEC (STEC) to vertical TEC (VTEC) using a suitable mapping function S(E), given by [*Mannucci et al.*, 1993]

$$S(E) = \frac{1}{\cos(z)} = \left\{ 1 - \left(\frac{R_E \times \cos(E)}{R_E + h_S} \right)^2 \right\}^{-0.5} \quad (4)$$

with

z = zenith angle of the satellite as seen from the observing station,

R_E = radius of the Earth,
E = the elevation angle in radians, and
h_s = the altitude of the thin layer above the surface of the Earth (taken as 350 km)

[15] We computed the rate of change of TEC (ROT) over 30-s intervals using measurements of relative TEC. *Zou and Wang* [2009] explained that increased ROT indices have been utilized to investigate the irregularity in plasma bubbles and to study the evolution of large scale irregularities at scale lengths of a few kilometers. Only data corresponding to raypath elevations above 20° were used to reduce the impact of multipath.

3. Results and Discussion

[16] Figures 1a–1g show the month-to-month corrected amplitude scintillation (S_4) of all observed GPS satellites as a function of universal time (UT) (LT = UT + 1 h) from February to August 2010. S_4 is around 0.1 most of the time.
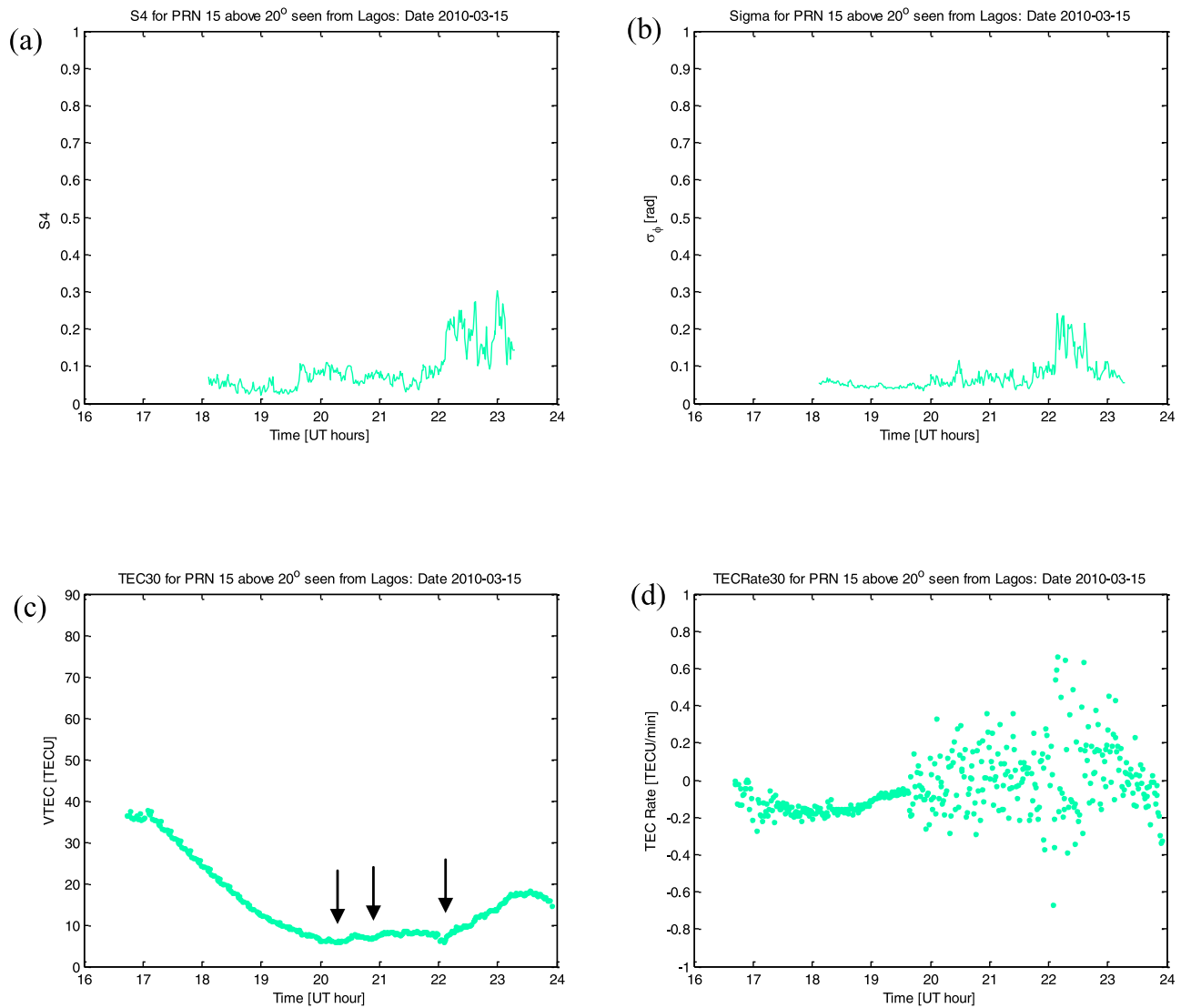
Figure 6. Plots of (a) S_4, (b) sigma, (c) VTEC, and (d) TEC rate for PRN 15 (LT = UT + 1 h). (The arrow indicates the presence of plasma bubble.)

This is due to the ionosphere since the effect of multipath has been removed. It is found that amplitude scintillation events are not only a nighttime phenomenon, but can also occur during the day in all the months considered. In general, the S_4 index increased during post-sunset hours. However, daytime amplitude scintillation with S4 > 0.4 occurred in some months. Several authors credit the generation of post-sunset irregularities in the equatorial ionosphere to the Rayleigh Taylor Instability (RTI) mechanism [*Abdu et al.*, 1981; *Abdu*, 2001; *Sultan*, 1996; *Basu et al.*, 1996; *Siefring et al.*, 2011]. The post-sunset equatorial enhancement of upward *F* region drift [*Fejer et al.*, 1979] pushes the height of the maximum electron density in the F layer to higher altitudes and thereby increases the percentage occurrence of scintillations in the equatorial region. According to *Zou and Wang* [2009], daytime scintillations are caused by small irregularities in the ionospheric E region.

[17] We established from the analysis of several days of observations that enhanced nighttime amplitude scintillations always occurred with enhanced nighttime phase scintillations

and TEC fluctuations at Lagos. As an example, Figures 2a–2d illustrate the amplitude scintillation index (S_4), phase scintillation index (σ_φ), VTEC and ROT observed at Lagos on 1 February 2010, a typical equatorial non-scintillation day. The S_4 index is generally below 0.2, whereas an S_4 index of 0.4 and above is indicative of scintillation events. There are no incidents of large scale VTEC depletions or rapid TEC fluctuation during this period of weak amplitude and phase scintillation events. From Figure 2a it is clear that no satellite signals experience scintillation activity ($S_4 > 0.2$) during the day time. However, Figure 3 shows that the presence of some large scale depletions of VTEC or plasma bubbles may be noted during the post-sunset hours between 20:00 UT (21:00 local time) and 23:00 UT (00:00 local time) on 15 March 2010. The depleted density of the ionosphere inside the volume of the bubble very often produces rapid changes both in amplitude and phase of the trans-ionospheric signals [*Dandekar and Groves*, 2004; *Strangeways et al.*, 2011; *Gherm et al.*, 2011]. *Zou and Wang* [2009] explained that the TEC depletions are plasma bubbles. *Zernov et al.*
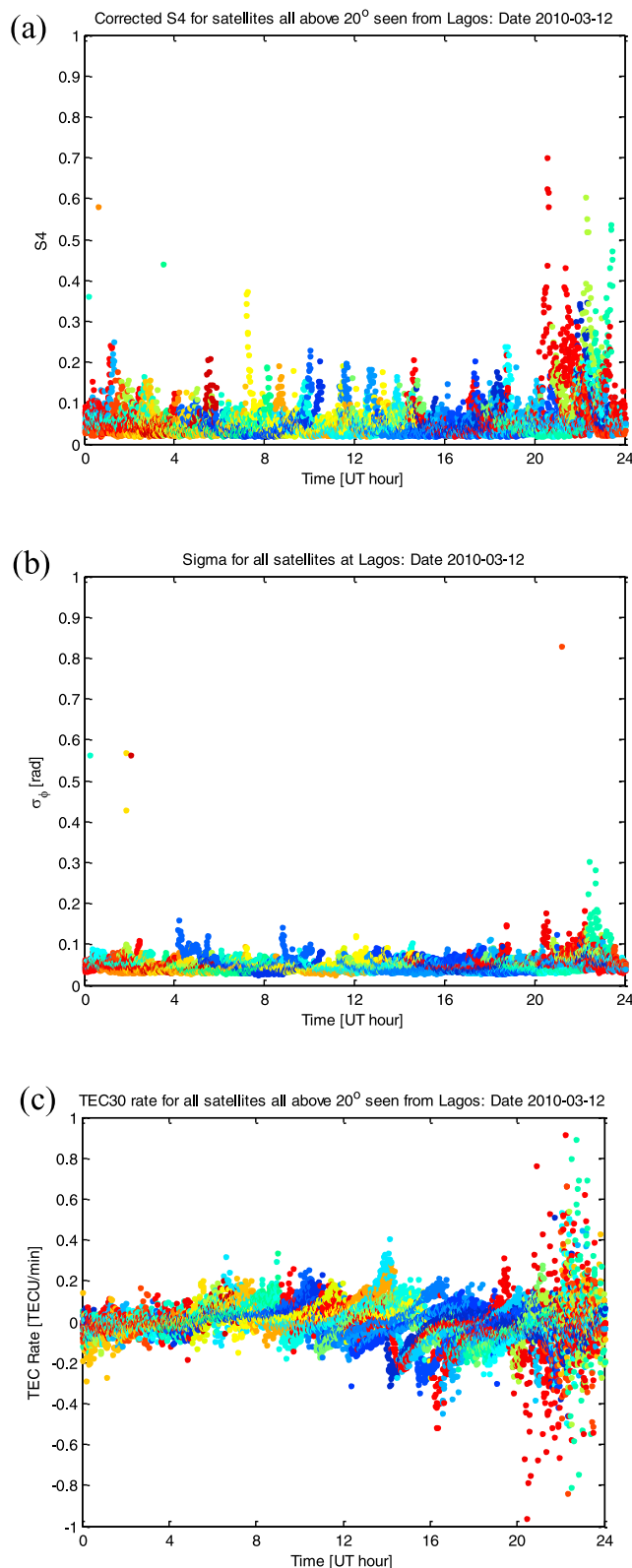
Figure 7. Plots of (a) S$_4$, (b) sigma, and (c) TEC rate for 12 March 2010 (LT = UT + 1 h).

[2009] studied the effects of scintillation of low-latitude bubbles on transionospheric paths of propagation. Their result showed that strong enhancements of S$_4$ are related to the bubbles. In order to show the relationship between increased S$_4$ structures and VTEC depletion (hence plasma bubbles), we included VTEC change plots along selected individual satellite passes. Figures 4, 5 and 6 show the S$_4$, σ_φ, VTEC and ROT measurements from GPS satellites, PRN 5, PRN 10, and PRN 15, observed on the night of 15 March 2010 during 16:00 UT and 24:00 UT. The arrows in Figures 4–6 indicate the presence of plasma bubbles. A close comparison of these figures indicates that TEC depletions correspond to increased fluctuations of ROT. This establishes that plasma bubbles are associated with large scale irregularities at scale length of a few kilometers. It may be concluded that the enhanced scintillation structures of S$_4$ and sigma, detected shortly after 20:00 UT, correspond quite well with TEC depletions and ROT fluctuations.

[18] Figure 7 compares the temporal structures of S$_4$, σ_φ, and ROT obtained from the all GPS satellites, observed at Lagos on 12 March 2010. Comparing Figure 7a with Figures 7b and 7c, it is obvious that the enhanced scintillation (S$_4$) structure, detected shortly after 20:00 UT, correspond quite well with ROT fluctuations and enhancement of σ_φ.

[19] The result of this work shows that nighttime amplitude scintillations always occurred with phase scintillations and TEC fluctuations at Lagos. *Zou and Wang* [2009] reported a similar result that the nighttime amplitude scintillations observed at Gulin (25.3°N, 110.3°E) always occurred with phase scintillations, TEC depletions, and ROT fluctuations.

[20] Hourly global TEC maps for 1st February 2010 are shown in Figure 8 and hourly global TEC maps for 15th March 2010 are shown Figures 9, 10, and 11. The maps were created using MIDAS (Multi-Instrument Data Analysis System) [*Mitchell and Spencer*, 2003; *Spencer and Mitchell*, 2007]. As expected, there are not really any high TEC values throughout the day of 1st February 2010 (Figure 8). This coincides with low S$_4$ values, as shown in Figure 2a. Hourly global TEC maps for 15th March 2010 show higher TEC values than the non-scintillation day (1st February 2010). Figures 9 and 10 show that large-scale ionospheric structure evolves across Nigeria from 12:00 UT to approximately 19:00 UT. There are smaller-scale structures around 20:00 UT and 22:00 UT (Figure 11). This suggests that there may be a link between the large scale structures in the afternoon and the scintillation effects later on, between 20:00 UT and 24:00 UT as shown by the enhanced S$_4$ structure in Figure 3a.

[21] We have computed the percentage of scintillation occurrence observed for three distinct thresholds of scintillation; namely S$_4$ > 0.2, S$_4$ > 0.3 and S$_4$ > 0.4, as shown in Figures 12a–12e. The percentage occurrence is defined as the ratio of the number of minutes with scintillation for a particular threshold to the total minutes of observation. For all thresholds of scintillation, the maximum percentage occurrences are observed in March and April, the equinox months, around 20:00 UT–23:00 UT. An explanation of the equinox maxima, according to *Tsunoda* [1985], is that scintillation maximizes at times of the year when the solar terminator is most nearly aligned with geomagnetic flux tubes, i.e., when the height-integrated *E* region Pedersen conductivity is
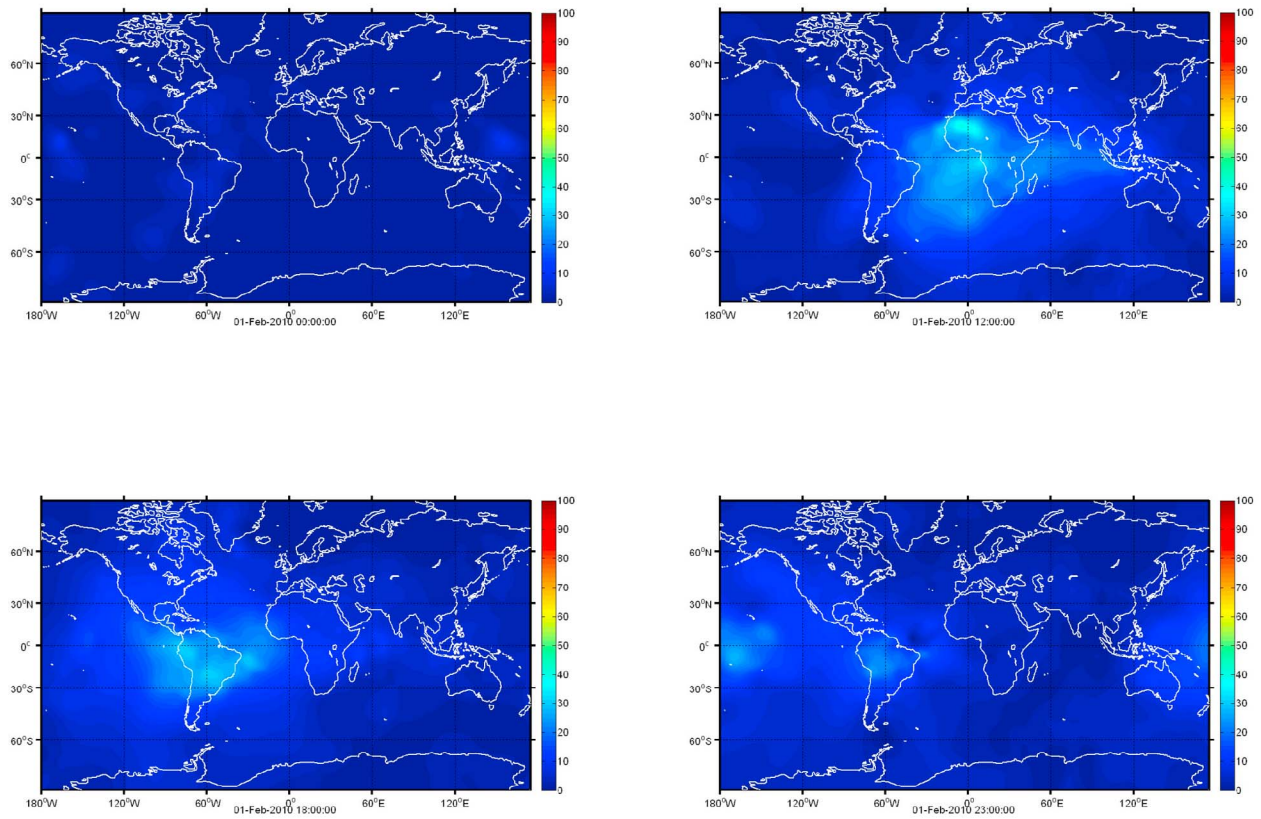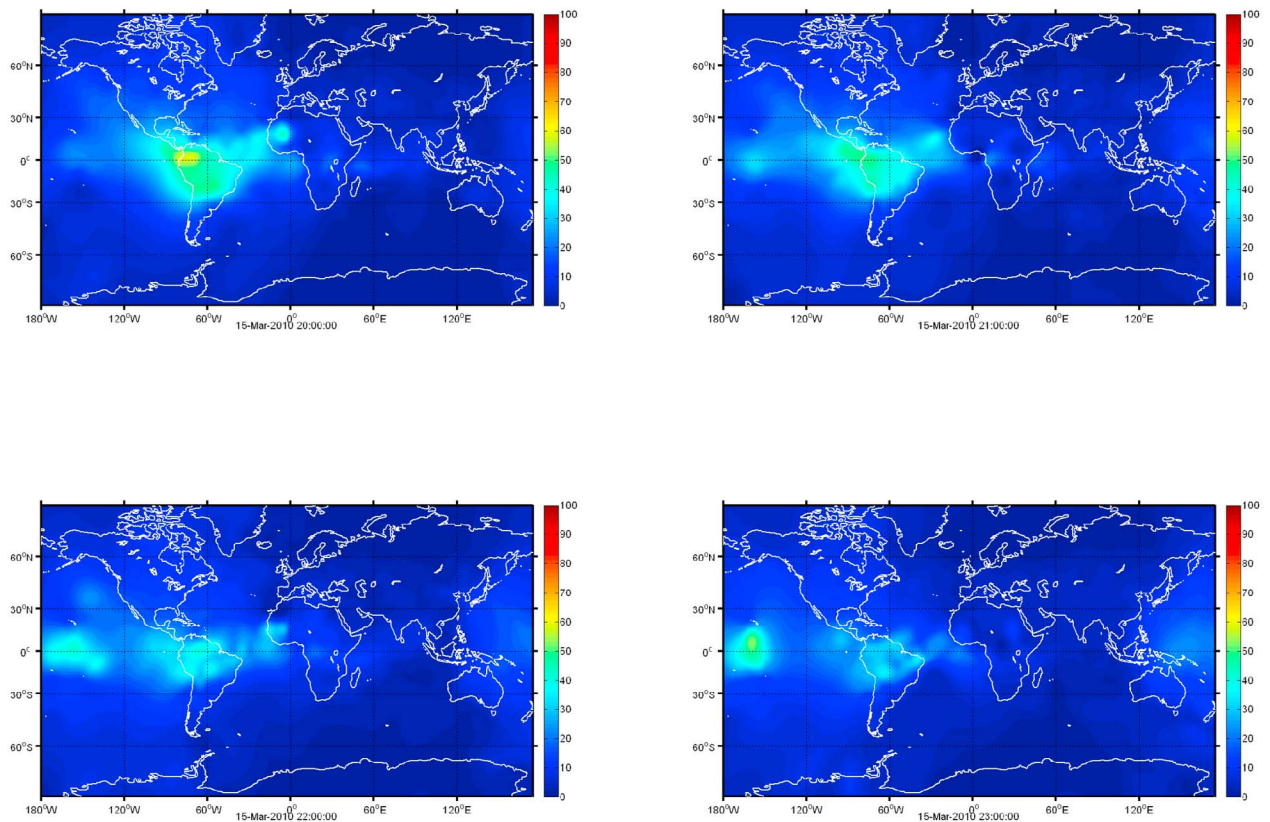
Figure 8. Hourly global TEC maps for selected hours on 1st February 2010.
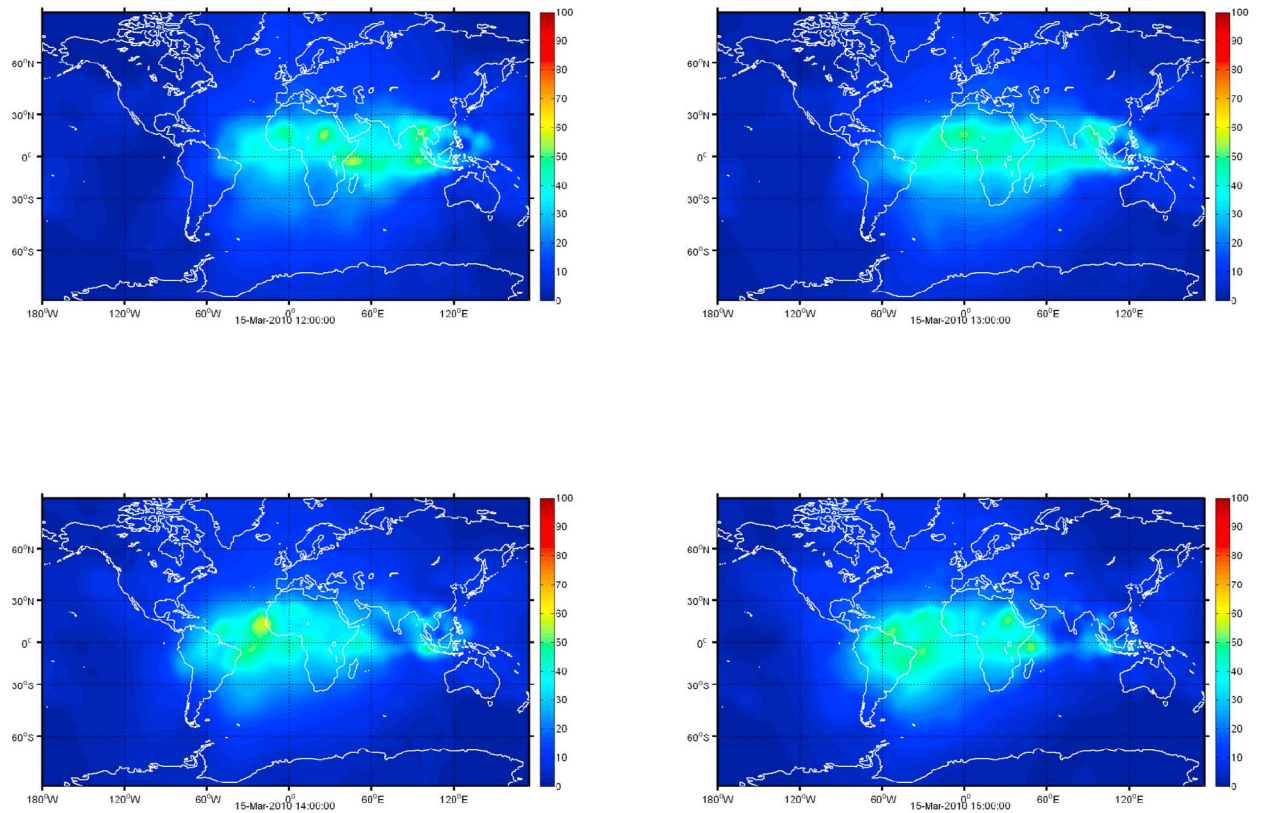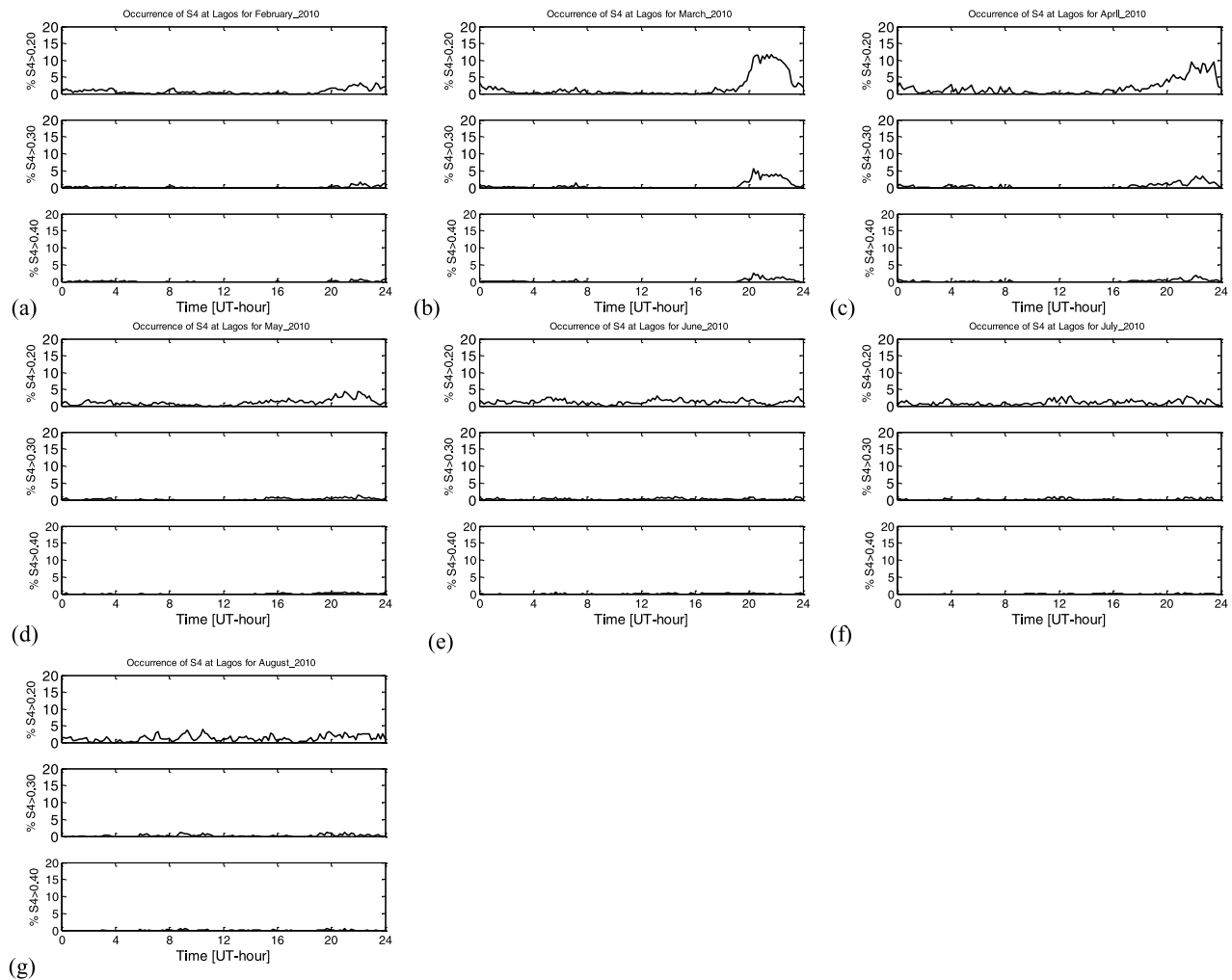

Figure 9. Hourly global TEC maps for 12:00 to 15:00 UT on 15th March 2010.
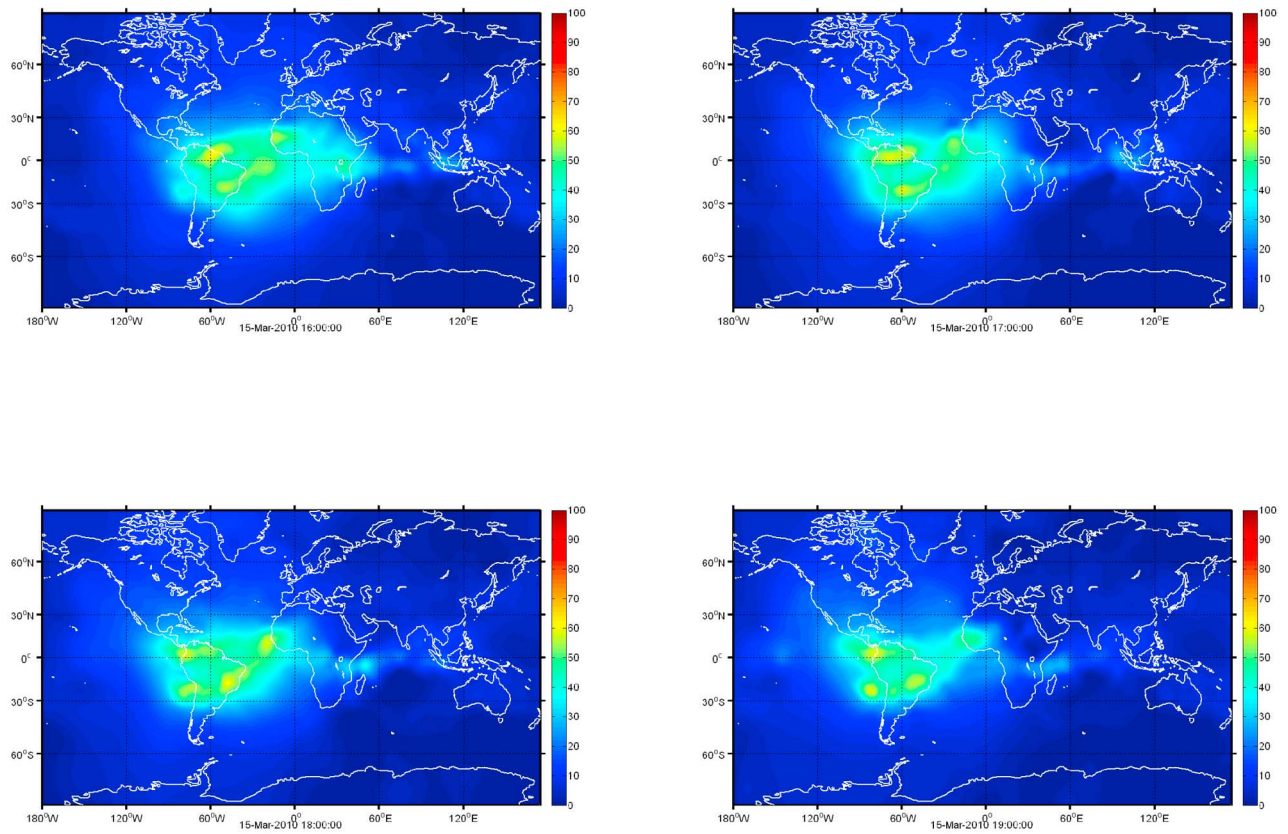
Figure 10. Hourly global TEC maps for 16:00 to 19:00 UT on 15th March 2010.

Figure 11. Hourly global TEC maps for 20:00 to 23:00 UT on 15th March 2010.

Figure 12. Diurnal and seasonal variation of percentage occurrence of scintillations during February 2010 to August 2010 (LT = UT + 1 h).

changing most rapidly. The percentage occurrence for scintillations with S_4 larger than 0.4 is rarely observed in all the months under consideration except in March and April. The conclusion to be drawn is that a seasonal pattern exists in percentage occurrence of scintillation activity over Lagos, although we need to extend the scintillation database before we can make a generalized statement on the seasonal variation of scintillation activity over Lagos.

4. Conclusion

[22] A preliminary study on ionospheric scintillation and TEC variation at Lagos has been carried out using GPS measurements between February 2010 and August 2010. The main results of the investigation are summarized as follows:

[23] 1. Amplitude scintillation events may occur during the day in all the months considered. In general, the S_4 index increased during post-sunset hours.

[24] 2. Enhanced amplitude scintillation (S_4) and phase scintillation (σ_φ) correspond quite well with TEC depletions and increased ROT and that nighttime amplitude scintillation

always occurred together with phase scintillation and TEC fluctuation at Lagos.

[25] 3. There is a link between the large scale structures in the afternoon and the equatorial evening scintillation effects.

[26] 4. The percentage occurrence of weak scintillation activity over Lagos, shows a clear seasonal pattern with peaks during equinoxes.

References

Aarons, J., M. Mendillo, and R. Yantosca (1996), GPS phase fluctuations in the equatorial region during the MISETA 1994 campaign, *J. Geophys. Res.*, *101*(A12), 26,851–26,862, doi:10.1029/96JA00981.

Abdu, M. A. (2001), Outstanding problems in the equatorial ionosphere-thermosphere electrodynamics relevant to spread F, *J. Atmos. Sol. Terr. Phys.*, *63*, 869–884, doi:10.1016/S1364-6826(00)00201-7.

Abdu, M. A., J. A. Bittencourt, and I. S. Batista (1981), Magnetic declination control of the equatorial F region dynamo electric field development and spread F, *J. Geophys. Res.*, *86*(A13), 11,443–11,446, doi:10.1029/JA086iA13p11443.

Abdu, M. A., E. A. Kherani, I. S. Batista, and H. A. Sobral (2009), Equatorial evening prereversal vertical drift and spread F suppression by disturbance penetration electric fields, *Geophys. Res. Lett.*, *36*, L19103, doi:10.1029/2009GL039919.

Andreeva, E. S., S. J. Franke, K. C. Yeh, and V. E. Kunitsyn (2000), Some features of the equatorial anomaly revealed by ionospheric tomography, *Geophys. Res. Lett.*, *27*(16), 2465–2468, doi:10.1029/1999GL003725.

Basu, Su., and S. Basu (1985), Equatorial scintillations: Advances since ISEA-6, *J. Atmos. Sol. Terr. Phys.*, *47*, 753–768, doi:10.1016/0021-9169(85)90052-2.

Basu, S., et al. (1996), Scintillations, plasma drifts, and neutral winds in the equatorial ionosphere after sunset, *J. Geophys. Res.*, *101*, 26,795–26,809, doi:10.1029/96JA00760.

Basu, S., K. M. Grooves, J. M. Quinn, and P. Doherty (1999), A comparison of TEC fluctuations and scintillations at Ascension Island, *J. Atmos. Sol. Terr. Phys.*, *61*(16), 1219–1226, doi:10.1016/S1364-6826(99)00052-8.

Dabas, R. S., and L. Kersley (2003), Study of mid-latitude nighttime enhancement in *F* region electron density using tomographic images over UK, *Ann. Geophys.*, *21*(12), 2323–2328, doi:10.5194/angeo-21-2323-2003.

Dandekar, B. S., and K. M. Groves (2004), Using ionospheric scintillation observations for studying the morphology of equatorial ionospheric bubbles, *Radio Sci.*, *39*, RS3010, doi:10.1029/2003RS003020.

Doherty, P., E. Ra, J. Klobuchar, and M. B. El-Arini (1994), Statistics of time rate of change of ionospheric range delay, in *Proceedings of ION GPS-94*, part 2, pp. 1589–1598, Inst. of Navig., Manassas, Va.

Dubey, S., R. Wahi, and A. K. Gwal (2006), Ionospheric effects on GPS positioning, *Adv. Space Res.*, *38*(11), 2478–2484, doi:10.1016/j.asr.2005.07.030.

Fejer, B. G., D. T. Farley, R. F. Woodman, and C. Calderon (1979), Dependence of equatorial F region vertical drifts on season and solar cycle, *J. Geophys. Res.*, *84*(A10), 5792–5796, doi:10.1029/JA084iA10p05792.

Gherm, V. E., N. N. Zernov, and H. J. Strangeways (2011), Effects of diffraction by ionospheric electron density irregularities on the range error in GNSS dual-frequency positioning and phase decorrelation, *Radio Sci.*, *46*, RS3002, doi:10.1029/2010RS004624.

Groves, K. M., et al. (1997), Equatorial scintillation and systems support, *Radio Sci.*, *32*, 2047–2064, doi:10.1029/97RS00836.

Huang, C. Y., W. J. Burke, J. S. Machuzak, L. C. Gentile, and P. J. Sultan (2001), DMSP Observations of equatorial plasma bubbles in the topside ionosphere near solar maximum, *J. Geophys. Res.*, *106*(A5), 8131–8142, doi:10.1029/2000JA000319.

Mannucci, A. J., B. D. Wilson, and C. D. Edwards (1993), A new method for monitoring the Earth's ionosphere total electron content using the GPS global network, in *Proceedings of ION GPS-93*, pp. 1323–1332, Inst. of Navig., Manassas, Va.

Mitchell, C. N., and P. S. J. Spencer (2003), A three-dimensional time-dependent algorithm for ionospheric imaging using GPS, *Ann. Geophys.*, *46*(4), 687–696.

Mitchell, C. N., L. Kersley, J. A. T. Heaton, and S. E. Pryse (1997), Determination of the vertical electron-density profile in ionospheric tomography: Experimental results, *Ann. Geophys.*, *15*, 747–752, doi:10.1007/s00585-997-0747-1.

Siefring, C. L., P. A. Bernhardt, D. E. Koch, and I. J. Galysh (2011), Using TEC and radio scintillation data from the CITRIS radio beacon receiver to study low and mid-latitude ionospheric irregularities, *Radio Sci.*, *46*, RS0D19, doi:10.1029/2010RS004585.

Spencer, P. S. J., and C. N. Mitchell (2007), Imaging of fast moving electron-density structures in the polar cap, *Ann. Geophys.*, *50*, 427–434.

Strangeways, H. J., Y. Ho, M. H. O. Aquino, Z. G. Elmas, H. A. Marques, J. F. G. Monico, and H. A. Silva (2011), On determining spectral parameters, tracking jitter, and GPS positioning improvement by scintillation mitigation, *Radio Sci.*, *46*, RS0D15, doi:10.1029/2010RS004575.

Sultan, P. J. (1996), Linear theory and modeling of the Rayleigh-Taylor instability leading to the occurrence of equatorial spread F, *J. Geophys. Res.*, *101*(A12), 26,875–26,891, doi:10.1029/96JA00682.

Tsunoda, R. T. (1985), Control of the seasonal and latitudinal occurrence of equatorial scintillation by the longitudinal gradient of integrated *E* region Pedersen conductivity, *J. Geophys. Res.*, *90*(A1), 447–456, doi:10.1029/JA090iA01p00447.

Wanninger, L. (1993), Ionospheric monitoring using IGS data, paper presented at the 1993 Berne IGS Workshop, Int. GPS Serv. for Geodyn., Berne, Switzerland, 25–26 March.

Wernik, A. W., J. A. Secan, and E. J. Fremouw (2003), Ionospheric irregularities and scintillation, *Adv. Space Res.*, *31*(4), 971–981, doi:10.1016/S0273-1177(02)00795-0.

Zernov, N. N., V. E. Gherm, and H. J. Strangeways (2009), On the effects of scintillation of low- latitude bubbles on transionospheric paths of propagation, *Radio Sci.*, *44*, RS0A14, doi:10.1029/2008RS004074.

Zou, Y., and D. Wang (2009), A study of GPS ionospheric scintillations observed at Guilin, *J. Atmos. Sol. Terr. Phys.*, *71*, 1948–1958, doi:10.1016/j.jastp.2009.08.005.

A. B. Adeloye, A. O. Adewale, and E. O. Oyeyemi, Department of Physics, University of Lagos, Lagos 234, Nigeria. (olajide3000@yahoo.com)

C. N. Mitchell and J. A. R. Rose, Invert Centre for Imaging Science, Department of Electronic and Electrical Engineering, University of Bath, Bath BA2 7AY, UK.

P. J. Cilliers, SANSA Space Science, PO Box 32, Hermanus 7200, South Africa.